Proceedings of the 21st ICSMGE, Vienna, Austria, 14 – 19 June 2026. Pistrol, Adam & Schweiger (eds.)
Published by: ÖGG, Austrian Society for Geomechanics, Salzburg, Austria, ISBN 978-3-9503898-4-5
https://doi.org/10.53243/ICSMGE2026-608

Sensitivity analysis of building features on damage induced by shallow tunnelling in soft ground

Hozaifa K. E. Ahmed, **Emilio Bilotta**
Department of Civil, Architectural and Environmental Engineering, University of Napoli Federico II, Naples, Italy, emilio.bilotta@unina.it

Marialuigia Sangirardi
Department of Engineering Science, University of Oxford, Oxford, UK

ABSTRACT: This study investigates the sensitivity of masonry building façades to damage induced by shallow tunnelling in soft ground. A three-dimensional finite element model is developed to explore the influence of key structural and geotechnical features. The analysis focuses on the effects of foundation geometry (specifically width, ground-to-foundation clearance, and embedment depth) as well as the tunnel's horizontal eccentricity and depth relative to the building. The variation of soil stiffness is also considered to assess its impact on damage levels. Façades are modelled accounting for the nonlinear constitutive behaviour of masonry. Results are compared with those obtained using a linear elastic hypothesis for the structure to highlight the importance of realistic modelling assumptions. Tunnel excavation is simulated via a single-step volume loss method, and damage is assessed using a characteristic tensile strain criterion that accounts for stress concentrations that typically occur around openings. The results demonstrate that both foundation geometry and tunnel location significantly influence the distribution and magnitude of tensile strains within the façade. Notably, increasing foundation width and embedment depth may intensify damage. In contrast, increasing the horizontal and vertical distance between the tunnel and the building consistently reduces damage. Furthermore, stiffer soil conditions are shown to increase tensile strain levels. These findings reveal the complex interaction between building configuration, tunnelling parameters, and soil properties. The insights gained can inform more effective risk mitigation strategies during the planning and execution of tunnelling projects in urban environments.

KEYWORDS: urban tunnelling, finite element method (FEM), masonry buildings, damage assessment, sensitivity analysis.

1 INTRODUCTION

The expansion of underground infrastructures in urban environments, particularly through tunnelling, is a common practice aimed at addressing the growing demands for transportation and utilities. However, such activities inevitably induce ground deformations, leading to surface settlements that can significantly impact overlying structures. Among these, masonry buildings, especially those with historical and architectural significance, are highly susceptible to damage from tunnelling-induced ground movements (Boscardin & Cording, 1989). Understanding and accurately predicting the interaction between tunnelling-induced ground movements and existing structures is therefore paramount for ensuring urban development sustainability and preserving built heritage.

Previous research has extensively investigated the mechanisms of tunnelling-induced ground deformation and its effects on structures. Various analytical, empirical, and numerical methods have been developed to assess building response, ranging from simplified beam analogies (Burland, 1995; Mair et al., 1996; Potts & Addenbrooke, 1997) to more complex three-dimensional finite element analyses (Burd et al., 2000; Losacco et al., 2014; Bilotta et al., 2017; Boldini et al., 2018; Pascariello et al., 2023). Despite these advancements, challenges remain in accurately capturing the complex behaviour of masonry structures, assessing the influence of openings and the anisotropic material response, which are critical for realistic damage prediction. Furthermore, the sensitivity of structural response to key geotechnical and structural parameters often requires detailed investigation to inform design and mitigation strategies.

This study presents a comprehensive numerical assessment of damage induced by shallow tunnelling in soft ground on masonry structures. The primary objective is to investigate the influence of several key building and tunnelling features, including foundation geometry, tunnel position (both horizontal eccentricity and depth), and surrounding soil stiffness, on the resulting building damage. Advanced constitutive models, specifically the Hardening Soil Model with Small Strain (HS Small) (Benz et al., 2009) for soil and the Jointed Masonry Model (JMM) (Lasciarrea et al., 2019) for masonry, are employed to provide an accurate representation of material behaviour. Constitutive parameters for masonry are calibrated on existing literature (Ravenshorst et al., 2016; Esposito et al., 2016).

Starting from a reference ideal scenario, a systematic sensitivity analysis is conducted by varying these parameters, and their impact on the resulting building damage is rigorously assessed. Moreover, the study critically evaluates the applicability and limitations of different damage assessment methodologies, by comparing their predictions.

The insights gained are intended to contribute to the development of more reliable and robust methodologies for predicting and mitigating tunnelling-induced damage to masonry buildings in urban environments.

2 METHODOLOGY

This section outlines the numerical modelling approach adopted to investigate tunnelling-induced damage to masonry façades. The study builds upon the reference work by Amorosi & Sangirardi (2021), which examined the response of both full masonry buildings and isolated façades to tunnel excavation via numerical analyses performed in the commercial code PLAXIS 3D (Bentley Systems, 2024). That study also established a validated modelling setup, which is retained here to ensure consistency and comparability.

In the present work, the same soil domain dimensions are employed - 160 m in the x-direction, 20 m in the y-direction (parallel to the tunnel axis), and 50 m in the z-direction (depth) - to minimise boundary effects. The façade geometry, tunnel depth, and positioning are likewise consistent with the reference study and serve as the baseline for an extended parametric investigation.

This study introduces modified façade wall geometries to evaluate their influence on tunnelling-induced damage. In

addition to the reference façade, alternative configurations are analysed to assess the role of specific structural features. For simplification, only an isolated façade wall is modelled. Tunnel excavation is simulated using a single-step volume loss method.

To investigate the sensitivity to foundation geometry, the strip footing is varied in three features: width (1.0 m and 1.2 m), clear distance from ground surface to footing base (0.5 m, 1.0 m, and 1.5 m), and embedment depth (0.5 m, 1.0 m, and 1.5 m). The soil profile used in the reference study is maintained throughout all cases to isolate the structural variables as the primary factors affecting response.

Figure 1 illustrates the overall model geometry, including the façade, tunnel alignment, and soil boundaries.

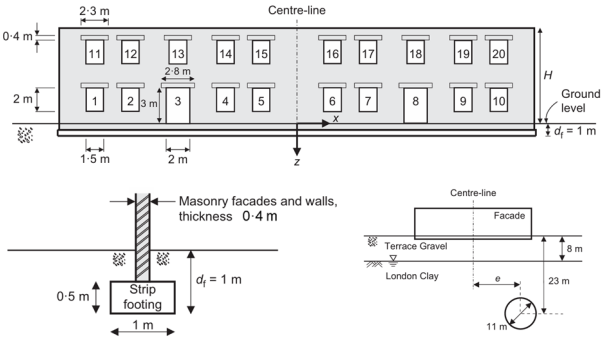

Figure 1. Model geometry showing façade, tunnel, and soil domain configuration (Amorosi & Sangirardi, 2021. Adapted from Yiu, Burd and Martin, 2017).

2.1 *Soil Constitutive Model: HS Small*

For the soil, the Hardening Soil Model with Small-Strain (HS Small) (Benz et al., 2009) is adopted to capture its non-linear stress-strain behaviour of soft ground, particularly at small strains relevant to tunnelling-induced deformations. This constitutive model captures the initial stiffness degradation with strain and provides a more realistic representation of soil response near the tunnel. The input parameters used for Terrace Gravel and London Clay were adopted from literature (Amorosi & Sangirardi, 2021) and are summarised in Table 1.

Table 1. HS small parameters.

Parameter	Terrace gravel	London Clay	Unit
G_0^{ref}	133	81.5	MPa
m	1	1	-
φ'	35	26	°
c'	0	5	KPa
Ψ	17.5	0	°
p^{ref}	100	100	KPa
$\gamma_{0.7}$	2.5×10^{-4}	2.5×10^{-4}	-
$\gamma_{cut\text{-}off}$	8.4×10^{-4}	8.0×10^{-4}	-
G_{ur}^{ref}	25.282	16.359	MPa
N	0.2	0.2	-
E_{ur}^{ref}	60.677	39.263	MPa
E_{50}^{ref}	20.226	13.088	MPa
E_{oed}^{ref}	16.181	10.470	MPa
OCR	30	30	-
K_0	0.425	0.560	-

2.2 *Structural Constitutive Models*

Two constitutive hypotheses are considered for masonry: Elastic Linear (EL) and Non-Linear (NL) façades.

2.2.1 *Elastic Linear (EL) Façade*

A reference linear elastic material model is used for comparison. It approximates the façade as an equivalent beam: a simplification frequently used in empirical or preliminary structure-soil interaction analyses.

The same elastic properties will also be assigned to the Jointed Masonry Model (JMM), facilitating a direct comparison between linear and nonlinear façade responses. The adopted parameters are summarised in Table 2.

Table 2. Elastic façade

Parameter	Value	Unit
γ	19.62	MPa
G^{ref}	833.0	MPa
ν	0.2	-

2.2.2 *Non-Linear (NL) Façade (Jointed Masonry Model)*

The nonlinear behaviour of masonry is simulated using the Jointed Masonry Model (JMM) (Lasciarrea et al., 2019), a constitutive model specifically developed to capture the anisotropic behaviour of masonry assemblies. The JMM implicitly accounts for masonry internal structure and for the occurrence of failure on either bed or head joints according to a frictional Mohr-Coulomb criterion with tension cut-off on pre-determined and fixed orientations. Plastic points, indicating locations where yield criterion is met, are adopted as additional damage descriptors.

Material parameters include the elastic properties of the continuum, joint friction, cohesion and tensile strength. These were calibrated based on existing literature (Ravenshorst et al., 2016; Esposito et al., 2016) and are summarised in Table 3.

Table 3. JMM Properties.

Parameter	Value	Unit
γ	19.62	MPa
G	833.0	MPa
ν	0.2	-
β	0.636	-
C_{mc}	1.0	MPa
σ_{mc}	1.0	MPa
ϕ_{mc}	40	°
ψ_{mc}	0	°
$c_{0,i}$	0.14	MPa
$\sigma_{0,i}$	1.0	MPa
$\phi_{0,i}$	23.27	°
$\psi_{0,i}$	0	°

2.3 *Tunnel Excavation Simulation Procedures*

The simulation consists of three distinct phases within PLAXIS 3D:

1. **Initial Geostatic Stress State:** established based on the soil's unit weight and the groundwater level (8 m bgl).
2. **Façade Installation:** the masonry façade and footing are activated, allowing for stress redistribution under gravity.
3. **Tunnel Excavation:** The tunnel is excavated in a single step by applying a homothetic contraction to the tunnel lining. A volume loss value of 1.5% is assumed, consistent

with previous studies (Dulake, 2011; Amorosi & Sangirardi, 2021).

3 SENSITIVITY ANALYSIS

This section presents a comprehensive sensitivity analysis of the impact of various parameters on damage experienced by masonry façades due to tunnelling-induced ground movements. The parameters under investigation include foundation geometry, tunnel positioning, and soil stiffness. both EL and NL façade models are analysed.

3.1 *Maximum and Characteristic Principal Tensile Strain*

After modelling both façades using PLAXIS 3D, it was found that the maximum tensile strain for the NL façade is 0.313%, while for the EL façade, it is 0.082%. Yiu et al. (2017) highlighted a significant challenge when façades feature openings, such as windows and doors, which induce stress concentrations at internal corners. These stress singularities can lead to computational instability in strain values during mesh refinement, complicating damage assessments. Traditional metrics that focus on maximum tensile strain (ε_t) thus become unreliable due to their mesh dependency. To address this, Yiu et al. introduced the concept of "characteristic strain". This approach quantifies damage severity using a strain threshold (ε_{99}^t), defined as the tensile strain value not exceeded across 99% of the façade area. By focusing on this quantity, the method minimises the influence of localised singularities, providing a more stable and reliable metric for assessing damage.

In this study, the characteristic tensile strain was identified following these steps: (i) strain values are extracted at all Gauss points; (ii) each strain value is associated to its corresponding tributary volume (i.e. one fourth of each element volume); (iii) strains are sorted from highest to lowest; (iv) volumes are summed up to 1% of the total volume of the façade. The lowest strain within that 1% volume is taken as the characteristic tensile strain, ε_{99}^t. For the NL façade is $\varepsilon_{99}^t = 0.137\%$, while for the EL façade, $\varepsilon_{99}^t = 0.030\%$: a diagrammatic representation is reported in Figure 2.

Figure 3 shows the distribution of maximum principal strains, limited at the characteristic value, for both NL and EL façades. Notably, in the NL façade, the strain concentrates at the top of the door, whereas in the EL façade, it follows the tensile bending strain inclination typical of a beam.

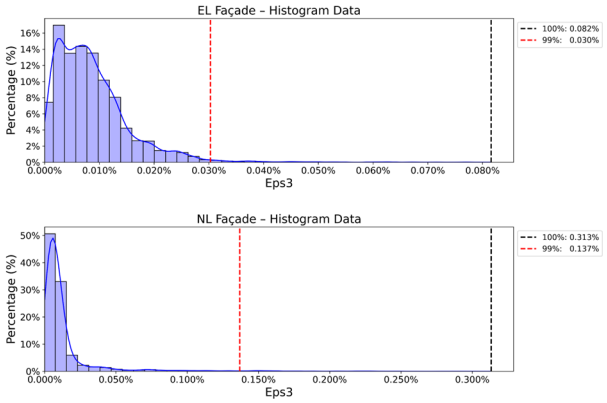

Figure 2. Percentage of point volume vs strain value for both NL and EL façades.

Figure 4 illustrates the excluded highest concentration tensile stress points that represent 1% of the total façade volume strain and their respective positions. It can be noted that most of these concentrations in the EL case occur at openings.

In Figure 5, plastic points for the NL case are depicted. These are distinguished between shear and tensile ones, indicating “where” the stress point has met the yield domain.

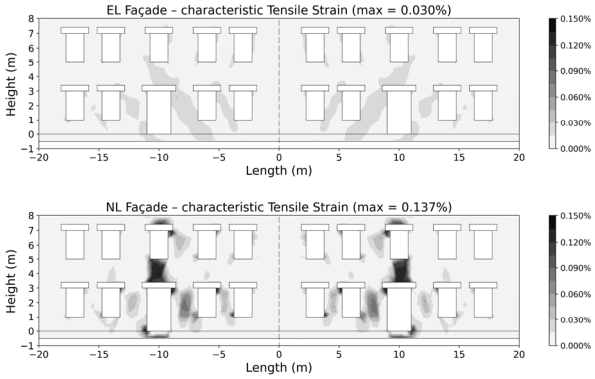

Figure 3. Distribution of maximum principal strain limited at the characteristic value, for both NL and EL façades.

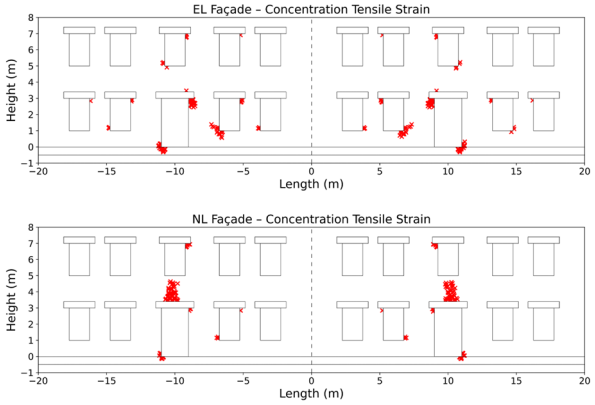

Figure 4. Excluded highest concentration tensile stress points that represent 1% of the total façade volume strain and their respective positions for both NL and EL façades.

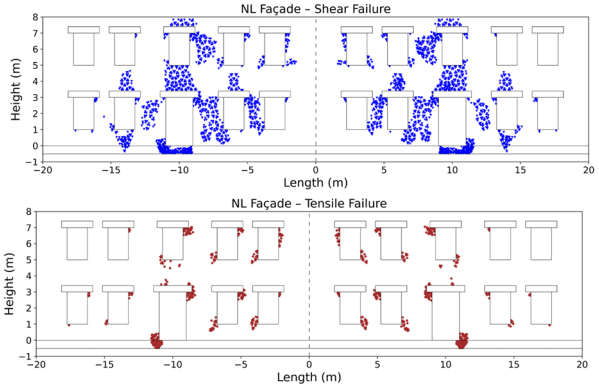

Figure 5. Plastic points on the interface for the NL façade.

3.2 *Damage Classification*

According to the damage categories defined by Boscardin and Cording (1989), the area above the door in the NL façade exhibits a characteristic tensile strain of 0.137%, classifying it as slight damage (category 2), which corresponds to strains between 0.075% and 0.15%. In contrast, the EL façade shows a characteristic tensile strain of 0.030%, placing it in the negligible damage category (category 0), associated with

strains between 0% and 0.05%. Figure 6 depicts the tensile strain distribution classified according to the damage categories metrics as per the colourbar on the right. While the EL case does not show any damage, under the same boundary conditions, the adoption of a NL constitutive hypothesis for masonry induces a different damage scenario.

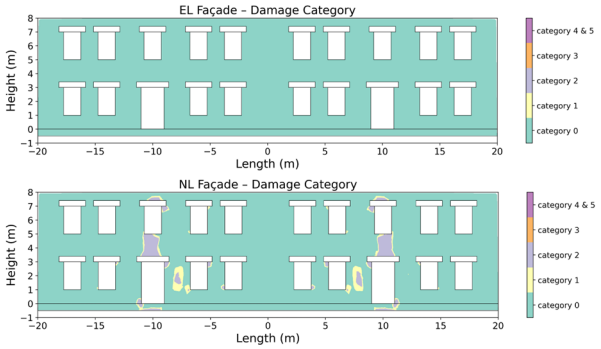

Figure 6. Façades damage categories for both NL and EL façades.

3.3 *Sensitivity to Foundation Geometry*

A first sensitivity analysis is performed to investigate the role of foundation geometry, by comparing the characteristic tensile strain experienced by the façade for different configurations, both in the NL and EL constitutive assumptions. The analysis involves systematic changes to the clear distance (d) between the ground surface and the footing, the embedment depth (D), and the footing width (T). Two widths are considered: 1.0 m (reference) and 1.2 m. The clear distance and embedment depth are examined at 0.5 m (reference), 1.0 m, and 1.5 m. The same soil profile used in the reference model is retained to ensure consistency and isolate the effects of structural variation.

Table 4 and Table 5 summarise the characteristic tensile strain for all façade configurations with varying footing geometries.

Table 4. Characteristic tensile strain for all Elastic Linear (EL) façades varying in footing geometry.

T		1.0 m		
d	D	0.5 m	1.0 m	1.5 m
0.5 m		0.030%	0.034%	0.037%
1.0 m		0.033%	0.036%	0.039%
1.5 m		0.036%	0.039%	0.041%
T		1.2 m		
d	D	0.5 m	1.0 m	1.5 m
0.5 m		0.032%	0.035%	0.038%
1.0 m		0.034%	0.038%	0.041%
1.5 m		0.037%	0.041%	0.043%

Table 5. Characteristic tensile strain for all Non-Linear (NL) façades varying in footing geometry.

T		1.0 m		
d	D	0.5 m	1.0 m	1.5 m
0.5 m		0.137%	0.140%	0.153%
1.0 m		0.143%	0.148%	0.173%
1.5 m		0.153%	0.164%	0.197%
T		1.2 m		
d	D	0.5 m	1.0 m	1.5 m
0.5 m		0.143%	0.146%	0.166%
1.0 m		0.152%	0.159%	0.193%
1.5 m		0.161%	0.179%	0.213%

As observed, the characteristic strain increases when either d or D increases. For the EL façade, the trend for both d and D is dependent solely on the total depth of the façade. Additionally, increasing the footing width also results in a corresponding increase in characteristic strain.

3.4 *Sensitivity to Tunnel Position*

A sensitivity analysis is carried out to assess how variations in tunnel position - both in terms of horizontal eccentricity and depth - affect the characteristic tensile strain on the façade. The reference façades (NL and EL) are compared with five additional configurations by altering the tunnel horizontal eccentricity (e) and depth (H). In the reference case, the tunnel is positioned at a depth of 23.0 m, directly beneath the façade (i.e., horizontal eccentricity e = 0 m).

The tunnel depth is then increased by one tunnel diameter (11.0 meters), resulting in two configurations at depths of 23.0 m and 34.0 m. Similarly, the horizontal eccentricity is adjusted by shifting the tunnel 11.0 m laterally, yielding eccentricities of 0 m and 11.0 m, respectively.

Table 6 presents the resulting characteristic tensile strain for all six façade configurations with varying tunnel positions.

Table 6. Characteristic tensile strain for all façades varying in tunnel position.

EL façade				NL façade			
H	e	0 m	11 m	H	e	0 m	11 m
23 m		0.030%	0.020%	23 m		0.137%	0.037%
34 m		0.021%	0.015%	34 m		0.044%	0.014%

As observed, increasing both the horizontal eccentricity and the depth of the tunnel generally leads to a reduction in the characteristic tensile strain experienced by the façades. This trend reflects the expected soil-structure interaction behaviour as the deformation effects reduce with distance from the tunnel.

3.5 *Sensitivity to Soil Stiffness*

The sensitivity of the characteristic tensile strain to variations in soil stiffness is evaluated by comparing the performance of the reference façades (NL and EL), sitting on a medium-stiffness soil (Soil-2) with two additional scenarios: a softer soil (Soil-1) and a stiffer soil (Soil-3). The stiffness parameters for each soil type are varied by one order of magnitude across the three cases. These are summarised in Table 7.

Table 7. Parameters for the different soil stiffness.

Parameter	Soil-1 (Soft)	Soil-2 (Medium)	Soil-3 (Stiff)
E_{50}^{ref} (kPa)	20.27×10^2	20.27×10^3	20.27×10^4
E_{oed}^{ref} (kPa)	16.18×10^2	16.18×10^3	16.18×10^4
E_{ur}^{ref} (kPa)	60.68×10^2	60.68×10^3	60.68×10^4
G_0^{ref} (kPa)	133.0×10^2	133.0×10^3	133.0×10^4

The corresponding characteristic tensile strain values for the NL and EL façades under each soil stiffness scenario are presented in Table 8.

Table 8. Characteristic tensile strain for both NL and EL façade varying in soil stiffness.

Soil	EL Façade	NL Façade
Soil-1 (Soft)	0.005%	0.005%
Soil-2 (Medium)	0.030%	0.137%
Soil-3 (Stiff)	0.042%	0.183%

As shown, increasing soil stiffness results in an increase in characteristic tensile strain for both façade models. This outcome shows the effect of relative stiffness: although the stiffer ground deforms less overall, the greater deformability of the structure compared to the ground leads the façade to undergo higher localised tensile strains under tunnelling-induced loading.

In summary, the sensitivity analyses indicate that both foundation geometry and tunnel positioning significantly

influence the characteristic tensile strain on masonry façades. Specifically, increasing the depth and width of foundations tends to increase tensile strains, while increasing the distance between the tunnel and the structure - either horizontally or vertically - reduces these strains. Additionally, stiffer soils are associated with higher tensile strains in the façades, emphasising the need to account for soil stiffness in tunnelling projects to accurately assess and mitigate potential damage to overlying structures.

4 DAMAGE ASSESSMENT

Three distinct damage assessment methodologies are employed to evaluate the potential impact of tunnelling-induced ground movements on masonry façades. These methods range from simplified empirical approaches to more computationally intensive hybrid techniques, each offering a different level of sophistication and capturing distinct aspects of the façade's structural response. By comparing the results derived from these approaches, the analysis aims to develop a comprehensive understanding of the resulting damage patterns and their sensitivity to key building features. This comparative evaluation also enables a critical appraisal of the applicability and limitations of each method within the context of shallow tunnelling in soft ground.

4.1 *Potts and Addenbrooke (1997) Method*

The Potts and Addenbrooke (1997) method offers a simplified analytical framework for assessing building damage due to ground movement. It models the building as an equivalent elastic beam and evaluates deformation using the deflection ratio and horizontal strain at foundation level. A modification factor is applied to account for the influence of the façade on the structure's stiffness. Despite its computational efficiency, this method is based on simplified assumptions and may not fully capture the complex behaviour of masonry, especially in façades with openings or heterogeneous material properties.

The implementation of this method involves the following steps:

- **Ground Movement Analysis**: The deflection ratio (Δ/L or DR) and the horizontal strain at the foundation level are derived from greenfield settlement results obtained from the numerical simulations. Separate values are calculated for hogging and sagging conditions.
- **Façade Property Definition**: Cross-sectional properties of the equivalent beam - namely the effective area A^* and moment of inertia I^*- are computed to reflect the influence of openings, following the approach by Pickhaver (2010). These are used to calculate the axial stiffness ratio α and the bending stiffness parameter ρ, which quantify the façade-to-soil stiffness ratio.
- **Application of Modification Factors**: Based on the calculated stiffness ratios, corresponding modification factors are extracted and applied to the deflection ratio and horizontal strain. This yielded adjusted values accounting for façade flexibility.
- **Damage Classification**: The final reduced values of deflection ratio and horizontal strain are evaluated against established thresholds to assign a damage category. In both hogging and sagging scenarios, the predicted damage is negligible (Category 0).

4.2 *Hybrid Tensile Strain Method*

The hybrid tensile strain method integrates numerically derived ground deformation data with established deflection-based damage criteria. Unlike empirical methods that approximate façade behaviour, this approach directly uses the settlement profile obtained from the numerical model to calculate deflection ratios and horizontal strains. As such, it provides a more physically grounded evaluation of potential building deformation and associated damage.

The procedure for this method includes the following steps:

- **Settlement Profile Extraction**: The ground surface settlement profile along the building foundation is extracted directly from the numerical results.
- **Deflection Ratio Calculation**: The local deflection ratio (DR) is determined by dividing the maximum differential settlement between two points along the façade by their separation distance. The highest value along the façade is taken as the governing DR. For the reference case, the calculated DR was 0.05% for hogging and 0.041% for sagging.
- **Horizontal Tensile Strain Calculation**: The curvature of the settlement profile is used to estimate the average horizontal tensile strain at the base of the façade. For the reference scenario, the resulting strain was 0.0005% for hogging and effectively zero for sagging.
- **Damage Category Assessment**: Based on the computed deflection ratio and tensile strain, damage levels are assigned using established strain-based thresholds. In this case, both hogging and sagging were classified as negligible damage (Category 0).

4.3 *Characteristic Tensile Strain Method:*

The characteristic tensile strain method evaluates damage based on the premise that when tensile strains in the masonry exceed specific thresholds, cracking and structural damage are likely to occur. This approach establishes a direct link between the material's tensile performance and the numerically obtained strain field, offering a more localized and physically representative assessment of damage potential.

The implementation procedure includes:

- **Limiting Tensile Strain ($\epsilon_{\mathbf{lim}}$) definition**: Damage categories are defined using threshold values of tensile strain, as proposed by Boscardin and Cording (1989).
- **Characteristic Tensile Strain Determination**: The characteristic tensile strain is obtained directly from the 3D numerical model, as described below, and is used for comparison against limiting thresholds.
- **Damage Category Assessment**: Damage levels are assigned by comparing the characteristic tensile strain to the corresponding ranges in Table 9. For the reference NL façade, the characteristic tensile strain of 0.137% falls within the range for Category 2 (slight damage). For the sagging scenario, where the characteristic strain was 0.0%, the damage classification is Category 0 (negligible damage).

Table 9. Damage categories limit (Boscardin & Cording, 1989).

Category of damage	Degree of severity	ε_{lim} (%)
0	negligible	0 – 0.05
1	very slight	0.05 – 0.075
2	slight	0.075 – 0.15
3	moderate	0.15 – 0.3
4 – 5	severe to very severe	> 0.3

4.4 *Summary and Comparative Analysis*

A summary of the damage assessment results obtained using the three methods - Potts & Addenbrooke (1997), Hybrid Tensile Strain, and Characteristic Tensile Strain - is presented in Table 10. The analysis considers both hogging and sagging deformation scenarios for the reference case, in which the

façade is located directly above the tunnel axis, with a footing depth of 1.0 m and a tunnel depth of 23.0 m.

Table 10. Damage Assessment Results for Reference Case.

Case	Potts & Addenbrooke	Hybrid Tensile Strain	Characteristic Tensile Strain
DR (hog)	0.003%	0.050%	N/A
ε_h (tens.)	0.0003%	0.0005%	N/A
ε_{99}^t	N/A	N/A	0.137%
Category	0 (Negligible)	0 (Negligible)	2 (Slight)
DR (sag)	0.0018%	0.041%	N/A
ε^h (comp.)	0.0%	0.0%	N/A
ε_{99}^t	N/A	N/A	0.0%
Category	0 (Negligible)	0 (Negligible)	0 (Negligible)

Note: DR = Deflection Ratio, ε_h = Horizontal Tensile Strain.

The results highlight key differences among the assessment methods. For both hogging and sagging, the Potts & Addenbrooke and Hybrid methods consistently classify the damage as negligible (Category 0). In contrast, the Characteristic Tensile Strain method indicates slight damage (Category 2) in the hogging scenario.

5 CONCLUSIONS

This study provides valuable insights into the sensitivity of masonry building façades to tunnelling-induced deformations. The numerical simulations consistently demonstrated that buildings located closer to the tunnel axis experience higher damage levels, aligning with expected ground deformation patterns. A key finding was the seemingly counterintuitive observation that increasing the footing depth led to increased damage, suggesting a more complex interaction with the ground deformation zone that deserves further investigation. Conversely, increasing the tunnel depth effectively reduced damage, as anticipated due to diminished surface settlements. Furthermore, the analysis highlighted that increased soil stiffness, while potentially reducing overall settlement, can lead to sharper settlement gradients, thereby increasing characteristic tensile strains and damage in the façade.

The comparative analysis of the three damage assessment methodologies (Potts & Addenbrooke, Hybrid Tensile Strain, and Characteristic Tensile Strain) revealed notable discrepancies in damage predictions. The simplified Potts & Addenbrooke method and the Hybrid Tensile Strain method generally predicted negligible damage for the reference case, whereas the Characteristic Tensile Strain method indicated slight damage for hogging. This difference highlights that the simplified Potts & Addenbrooke method, due to its inherent assumptions regarding building representation, generally predicted lower damage levels compared to the more detailed hybrid and characteristic tensile strain approaches. The characteristic tensile strain method proved effective in identifying localised high strain concentrations, which are crucial for assessing masonry damage but may not be fully captured by methods relying solely on deflection ratios. The consistent application of the characteristic tensile strain concept proved instrumental in providing a more robust and mesh-independent measure of overall façade strain, mitigating the effects of stress singularities around openings.

The findings underscore the critical importance of considering specific building features, tunnel parameters, and soil properties in comprehensive damage assessments. The observed differences between the assessment methodologies highlight the need for careful selection and application of appropriate tools, acknowledging their respective strengths and limitations. Future work will extend the current model to complete building configurations, enabling a thorough investigation of out-of-plane behaviour and providing a more comprehensive understanding of the complex soil-structure interaction problem. Ultimately, this research contributes to the development of more reliable and robust methodologies for predicting and mitigating damage to masonry buildings in urban tunnelling projects, enhancing the safety and sustainability of underground infrastructure development.

6 ACKNOWLEDGEMENTS

We acknowledge financial support under the National Recovery and Resilience Plan (PNRR), Mission 4, Component 2, Investment 1.1, Call for tender No. 104 published on 2.2.2022 by the Italian Ministry of University and Research (MUR), funded by the European Union – NextGenerationEU– Project Title "Damage Analysis and Monitoring of Ancient structures interacting with Geotechnical Excavations" – CUP E53D23002560006.

7 REFERENCES

Amorosi, A. & Sangirardi, M. (2021). Coupled three-dimensional analysis of the progressive tunnelling-induced damage to masonry buildings: Is it always worth it? *Tunn. Undergr. Space Technol.*, 118, p.104173.

Bentley Systems (2024). *PLAXIS 3D 2024.3.* Delft, Netherlands.

Benz, T., Vermeer, P. A., & Schwab, R. (2009). A small-strain overlay model. *Int. J Num. Anal. Meth. in Geomechanics*, *33*(1), 25–44.

Bilotta, E., Paolillo, A., Russo, G., Aversa, S. (2017). Displacements induced by tunnelling under a historical building. *Tunn. Undergr. Space Technol.* 61, 221–232.

Boldini, D., Losacco, N., Bertolin, S., Amorosi, A. (2018). Finite element modelling of tunnelling-induced displacements on framed structures. Tunn. Undergr. Space Technol. 80, 222–231.

Boscardin, M. D., & Cording, E. J. (1989). Building Response to Excavation-Induced Settlement. *J. Geotech. Eng.*, *115*(1), 1–21.

Burd, H. J., Houlsby, G. T., Augarde, C. E., & Liu, G. (2000). Modelling tunnelling-induced settlement of masonry buildings. *Proc. ICE-Geotechnical Engineering*, 143(1), 17-29.

Burland, J.B. (1995). Assessment of risk of damage to buildings due to tunnelling excavation. In: *Proc. 1st Int. Conf. Earthq Geotech. Eng, IS Tokyo '95* (ed. K. Ishihara), pp. 1189–1201. Tokyo, Japan.

Duláke, J. (2011). Crossrail project: Managing ground settlement risk. *Proceedings ICE – Civil Engineering*, 164(5), 35–40.

Esposito, R., Messali, F., & Rots, J. (2016). *Tests for the Characterization of Replicated Masonry and Wall Ties*. Delft University of Technology.

Lasciarrea, W. G., Amorosi, A., Boldini, D., de Felice, G., & Malena, M. (2019). Jointed Masonry Model: A constitutive law for 3D soil-structure interaction analysis. *Engineering Structures*, *201*.

Losacco N., Burghignoli A., Callisto L. (2014) Uncoupled evaluation of the structural damage induced by tunnelling *Géotechnique*, 64 (8), 646 – 656

Mair, R.J., Taylor, R.N., Burland, J.B. (1996). Prediction of ground movements and assessment of risk of building damage due to bored tunnelling. In: *Geotechnical Aspects of Underground Construction in soft ground,* pp. 713–718.

Pascariello M.N., Luciano A., Bilotta E., Acikgoz S., Mair R. (2023) Numerical modelling of the response of two heritage masonry buildings to nearby tunnelling. *Tunn. Undergr. Space Technol.*, 131, art. no. 104845

Pickhaver, J. A., Burd, H. J., & Houlsby, G. T. (2010). An equivalent beam method to model masonry buildings in 3D finite element analysis. *Computers and Structures*, 88(19–20), 1049–1063.

Potts, D. M., & Addenbrooke, T. I. (1997). A structure's influence on tunnelling-induced ground movements. *Proceedings ICE - Geotechnical Engineering*, *125*(1), 109–125.

Ravenshorst, G., & Messali, F. (2016). *In-plane tests on replicated masonry walls*. Rep. C31B60-2, Delft University of Technology.

Yiu, W. N., Burd, H. J., & Martin, C. M. (2017). Finite-element modelling for the assessment of tunnel-induced damage to a masonry building. *Geotechnique*, *67*(9), 780–794.